

METHOD FOR DETERMINING THE KINEMATIC PARAMETERS OF LONGITUDINAL PASS ROLLING

E. I. Shifrin¹ and N. Yu. Kvitka²

UDC 621.774.352

A new generalized method for calculating the rolling radius is developed. It is based on an analysis of the real shape of the neutral line in the deformation zone provided that the workpiece in equilibrium under the forces applied to it. It is established that there can be four characteristic positions of the neutral line within the contact surface between the roll and the workpiece. The particular case where the neutral line lies in a plane parallel to the rolling axis and the calculated rolling radius is effective is considered. The actual and effective rolling radii in the case of plugless rolling of pipes in oval roll passes are calculated and compared. A best-fit formula for correcting the calculated values of the effective rolling radius is obtained.

Keywords: longitudinal rolling, rolling speed, rolling radius, neutral line, tube reduction.

The actual boundary (neutral line) between the forward-slip and backward-slip zones during longitudinal pass rolling is a spatial curve $y_n = y_n[x_n(z), z]$ whose horizontal projection onto the plane XOZ is a plane curve $x_n = x_n(z)$ (Fig. 1). The coordinate z_n at which $x_n(z_n) = 0$ is called a neutral point. If a cylindrical coordinate system is used, the angle θ_n at which $x_n(\theta_n) = 0$ (Fig. 2) is called a neutral angle [1]. The rolling speed v_1 depends on the rolling radius R_{rol} , which is related to z_n as follows (Fig. 2):

$$R_{\text{rol}} = R_i - \sqrt{R_{\text{pz}n}^2 - z_n^2}, \quad (1.1)$$

where R_i is the ideal roll radius (distance from the roll axis to the rolling axis), mm; $R_{\text{pz}n} = R_{\text{pz}}(z_n)$ is the radius of the roll pass at the neutral point ($z = z_n$).

When analytically determining the rolling radius R_{rol} , use is often made [2–4] of the assumption proposed by Anisiforov et al. in [5]: the plane separating the contact surface into forward-slip and backward-slip zones is parallel to the symmetry plane XOY of the roll pass. With this assumption, the effective neutral line is a spatial curve parallel to the plane XOY , and the horizontal projection of this line onto the plane XOZ is a straight line parallel to the rolling axis OX (Figs. 1 and 2).

The coordinate z_{ne} of the intersection point between the effective neutral line and the centerplane YOZ of the rolls is called the effective neutral point. The effective rolling radius is defined by

$$R_{\text{rol e}} = R_i - \sqrt{R_{\text{pz}}(z_{\text{ne}})^2 - z_{\text{ne}}^2}. \quad (1.2)$$

¹ National Metallurgical Academy of Ukraine, Dnipro, Ukraine; e-mail: shifrinei48@gmail.com.

² George Brown College, Toronto, Canada; e-mail: nataliya.kvitka@gmail.com.

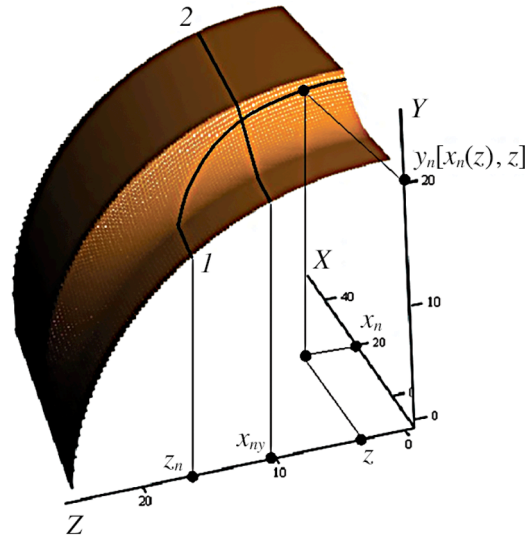


Fig. 1. Boundary between of forward-slip and backward-slip zones during longitudinal rolling: actual (1) and effective (2) neutral lines.

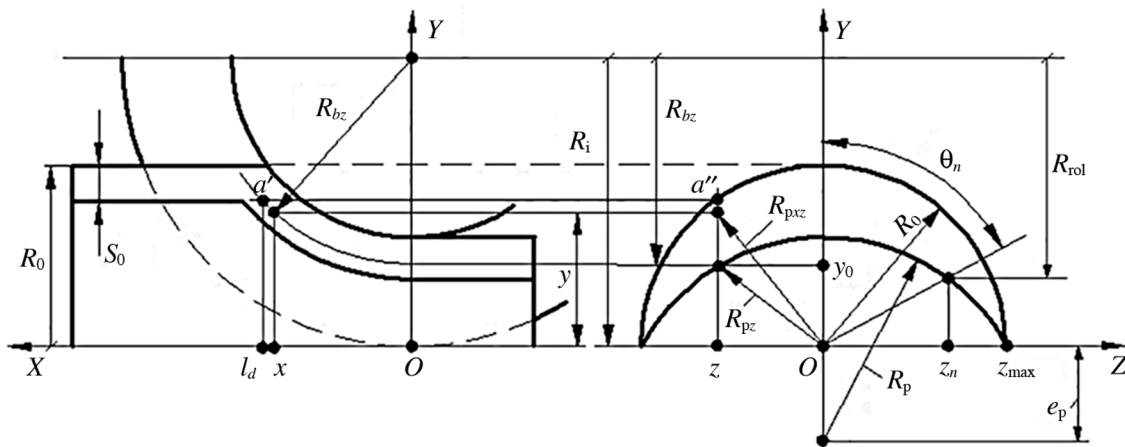


Fig. 2. Schematic of deformation zone.

Our Goal here is to compare the calculated values of the actual (R_{rol}) and effective ($R_{rol e}$) rolling radii in pass rolling.

Assumptions

To determine R_{rol} and $R_{rol e}$, we will assume that:

- a cylindrical (nonovalized) workpiece is rolled in rolls with equal geometrical parameters that rotate with equal angular velocities ω_r (as in simple longitudinal rolling of a strip [6]);
- there is no transverse metal flow on the pass surface (no widening), as in simple longitudinal rolling of a strip;

- the Bernoulli hypothesis holds: the current elongation μ in the deformation zone is averaged for each diametrical cross-section and is independent of the coordinates y and z ($\mu = \mu(x)$);
- the normal contact stress p is uniformly distributed over the contact surface between the metal and the roll ($p = p_{av}$);
- the normal (p) and tangential (τ) contact stresses are related by the Amontons–Coulomb law of friction $\tau = fp_{av}$ (where f is the coefficient of external contact friction).

Problem Statement

The velocity of the metal slipping over the roll is given by

$$\Delta v = v_c - v_{bz}, \quad (2)$$

where

$v_c = v_x \sqrt{1 - (x/R_{bz})^2}$ is the projection of the velocity v_x of the workpiece along the rolling axis onto the direction of the linear velocity v_{bz} of the roll surface,

$v_x = v_1 \mu_x / \mu_\Sigma$ is the velocity of the workpiece, m/sec,

$v_1 = \omega_r R_{rol}$ or $v_1 = \omega_r R_{rol y}$ is the velocity of the workpiece in the centerplane of rolls, m/sec,

$\mu_x = \mu_x(R_{mxav})$ is the current elongation, μ_Σ is the total elongation, $R_{mxav} = R_{mxav}(x)$ is the mean radius of the workpiece in a specific diametrical cross-section of the deformation zone with abscissa x , mm,

$R_{bz} = R_1 - \sqrt{R_{pz}^2 - z^2}$ is the current roll radius within the pass width, mm, $R_{pz} = R_{pz}(z)$ is the equation of the pass profile.

Let us determine the mean radius R_{mxav} of the workpiece. The perimeter of the workpiece as a function of its radius R_{mx} is determined from the equation

$$\Pi_x = 2n \int_0^{z_{max}} \sqrt{1 + \left[\frac{d(\sqrt{R_{mx}^2 - z^2})}{dz} \right]^2} dz, \quad (3)$$

where

$z_{max} = b \sin \pi/n$ is the maximum value of the coordinate z within the roll pass, n is the number of rolls forming the pass, b is the pass width, mm,

$R_{mx} = \begin{cases} R_x & \text{for } R_0 \geq R_x, \\ b & \text{for } R_0 < R_x \end{cases}$ is the current radius in the deformation zone,

$R_x = \sqrt{\left[R_1 - \sqrt{(R_1 - y_0)^2 - x^2} \right]^2 + z^2}$, $y_0 = y_0(z)$ is the ordinate of the point of the pass profile at the exit from the deformation zone determined from the equation of the pass profile, z is the coordinate of the point of the pass profile at the exit from the deformation zone.

The perimeter of the roll pass is expressed as $\Pi_p = 2\pi R_{mxav}$. Substituting it into Eq. (3) yields

$$R_{mxav} = \frac{n}{\pi} \cdot \int_0^{z_{max}} \sqrt{1 + \left[\frac{d(\sqrt{R_{mx}^2 - z^2})}{dz} \right]^2} dz.$$

The tangential contact stress τ is opposite to the velocity Δv ; therefore, in the forward-slip zone where $\Delta v > 0$, the elementary friction force $dT_{fw} = \tau dF_{fw}$ (where dF_{fw} is the area element of the contact surface in the forward-slip zone) applied to the workpiece is opposite to the rolling direction. In the backward slip zone where $\Delta v < 0$, the elementary friction force $dT_{bw} = \tau dF_{bw}$ (where dF_{bw} is the area element of the contact surface in the backward-slip zone) applied to the workpiece acts in the rolling direction.

It is obvious that the horizontal projection dP_x of the elementary normal pressure force $dP = p dF$ (where dF is the area element of the contact surface) is opposite to the rolling direction on all the contact surface.

Under the assumptions made above, the workpiece will be in equilibrium under all the forces $F_\Sigma = F_{fw} + F_{bw}$ applied to its contact surface along the rolling axis OX if

$$T_{fw} - T_{bw} + P_x + Q = 0, \tag{4}$$

where

$T_{fw} = \iint_{(F_{fw})} \tau n_{\tau x} dF$ is the resultant force along the rolling axis due to the elementary friction forces dT_{fw} in the forward-slip zone, kN,

$T_{bw} = \iint_{(F_{bw})} \tau n_{\tau x} dF$ is the resultant force along the rolling axis due to the elementary friction forces dT_{bw} in the backward-slip zone, kN,

$P_x = \iint_{(F_\Sigma)} p n_{px} dF$ is the resultant force along the rolling axis due to the elementary normal pressure forces dP , N,

$n_{\tau x}$ and n_{px} are the direction cosines of the projections of dT_{bw} , dT_{fw} and dP , respectively, onto the OX -axis,

Q is the external axial force applied to the workpiece, N.

The terms P_x and Q in Eq. (4) do not depend on the position of the neutral line in the deformation zone. The value of Q depends on the behavior of the external force: if $Q > 0$, the resultant external axial force is opposite to the rolling direction, and if $Q < 0$, then it is directed along rolling. If $p = p_{av}$, then P_x is determined

from the equation

$$P_x = 4np_{av}F_v, \tag{5}$$

where

$F_v = \int_0^{z_{max}} \left(R_{bz} - \sqrt{R_{bz}^2 - l_d^2} \right) dz$ is the projection of the contact surface area onto the centerplane YOZ ,
 $l_d = \sqrt{R_{bz}^2 - \left(R_i - \sqrt{R_0^2 - z^2} \right)^2}$ is the horizontal projection of the back boundary of the deformation zone onto the plane XOZ .

Calculation of Effective Rolling Radius

To calculate the effective rolling radius, the values of T_{fw} and T_{bw} in Eq. (4) are determined as follows:

$$T_{fw} = 4nfp_{av} \int_0^{z_{ne}} \frac{l_d}{\Phi} dz, \tag{6.1}$$

$$T_{bw} = 4nfp_{av} \int_{z_{ne}}^{z_{max}} \frac{l_d}{\Phi} dz, \tag{6.2}$$

where $\Phi = \cos \left(\arctan \frac{dy_0}{dz} \right)$.

Substituting (5), (6.1), and (6.2) into the force equilibrium equation (4), we resolve it for z_{ne} and use Eq. (1.2) to calculate the effective rolling radius R_{role} .

Calculation of Actual Rolling Radius

To calculate the actual rolling radius, the values of T_{fw} and T_{bw} in Eq. (4) are determined as follows:

$$T_{fw} = 4nfp_{aw} \int_0^{z_n} \frac{x_n(z, z_n)}{\Phi} dz, \tag{7.1}$$

$$T_{bw} = 4nfp_{aw} \int_0^{z_{max}} \frac{l_d - x_n(z, z_n)}{\Phi} dz. \tag{7.2}$$

The function $x_n(z, z_n)$, which is the projection of the actual neutral line onto the horizontal plane XOZ , is determined as the root of Eq. (2) at $\Delta v = 0$:

$$\left(R_i - \sqrt{R_{pzn}^2 - z^2} \right) \frac{\mu_x(x_n)}{\mu_\Sigma} \sqrt{1 - \left(\frac{x_n}{R_i - \sqrt{R_{pz}^2 - z^2}} \right)^2} - \left(R_i - \sqrt{R_{pz}^2 - z^2} \right) = 0. \tag{8}$$

When $R_{pz_n} = f(z_n)$, the solution of Eq. (8) is

$$x_n = x_n(z, z_n).$$

We will substitute this solution into Eqs. (7.1) and (7.2). Substituting (5), (7.1), and (7.2) into the force equilibrium equation (4), we resolve it for z_n and use Eq. (1.1) to calculate the actual rolling radius R_{rol} .

There are alternative ways to determine the coordinate z of the neutral point z_n . For example, the time it takes to calculate z_n becomes much shorter if we substitute (5), (6.1), and (6.2) into (4) to find z_{ne} and equate the right-hand sides of Eqs. (6.1) and (7.1) or Eqs. (6.2) and (7.2) to determine z_n .

Calculation Parameters

Consider the plugless rolling of pipes in an oval roll pass. Then

$$y_0 = \begin{cases} \sqrt{R_p^2 - z^2} - e_p, & \text{if } 0 \leq z \leq z_{max}, \\ \sqrt{R_p^2 - z_{max}^2} - e_p + \Psi(z), & \text{if } z_{max} < z, \end{cases} \tag{9}$$

where R_p and e_p are the radius and eccentricity of the roll pass (Fig. 2), $\Psi(z)$ is an arbitrary monotonically decreasing function.

The fictitious section $z > z_{max}$ is present in Eq. (9) because the position of the neutral line at which $z_n > z_{max}$ is possible. The form of the function $\Psi(z)$ affects the value of z_n for $z_n > z_{max}$, but not the value of the function $y_0(z_n)$ and the value of the rolling radius $R_{rol} = R_i - y_0(z_n)$, which do not depend on $\Psi(z)$. The linear function $\Psi(z) = z_{max} - z$ was used in the calculation. The equation of the oval profile of the roll pass is

$$R_{pz} = \sqrt{\left(\sqrt{R_p^2 - z^2} - e_p\right)^2 + z^2}. \tag{10}$$

In the calculation, the parameter $R_0 = b = 25 \cdot 10^{-3}$ m was used and the values of the following quantities were varied: $\lambda_p, f, \bar{R} = R_i/R_0, \bar{T} = R_0/R_0, \bar{Q} = Q/P_x$. The difference between R_{rol} and R_{role} was estimated using the ratio $U = R_{rol}/R_{role}$.

Calculated Results

Figure 3 shows the calculated parameters of the plane curve $x_n = x_n(z)$, which is a horizontal projection of the spatial curve $y_n = y_n[x_n(z), z]$ onto the plane XOZ .

From Fig. 3 it follows that there are four characteristic positions of the neutral line within the contact surface between the roll and the workpiece: 1 the neutral line crosses the x - and z -axes, 2 the neutral line crosses the z -axis and the back boundary of the contact surface, 3 the neutral line crosses twice the back boundary of the contact surface, 4 the neutral line crosses the x -axis and the back boundary of the contact surface. The conclusion that the neutral line can cross the x -axis and back boundary of the contact surface was drawn for

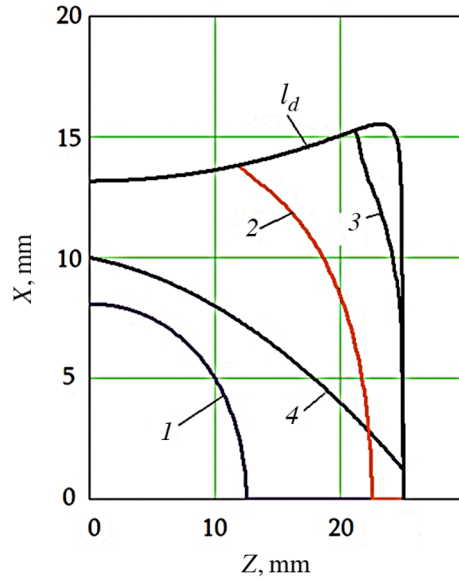


Fig. 3. Horizontal projections $x_n = x_n(z)$ of neutral lines for $n = 2$: 1 - $\bar{Q} = 1, f = 0.45$; 2 - $\bar{Q} = -0.75, f = 0.45$; 3 - $\bar{Q} = -1.5, f = 0.45$; 4 - $\bar{Q} = -0.6, f = 0.3$.

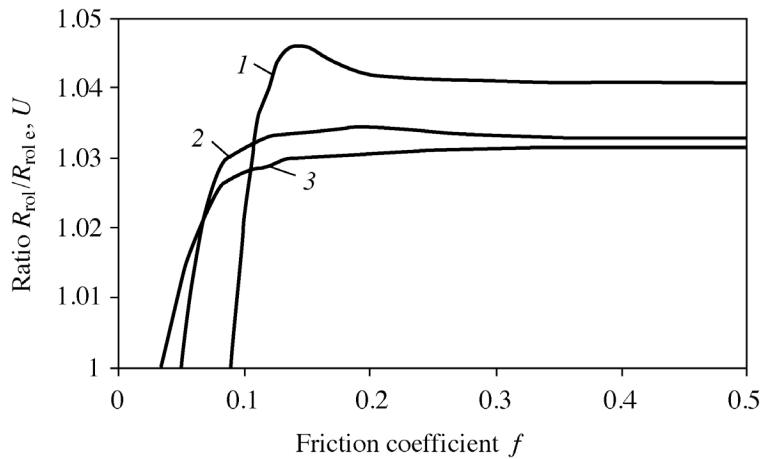


Fig. 4. Curves $U = U(f)$ for $\lambda_p = 1.05, \bar{Q} = 0, \bar{T} = 0.45, n = 2$: 1 - $\bar{R} = 2$; 2 - $\bar{R} = 5$; 3 - $\bar{R} = 10$.

the first time. In [11, 12] it was stated that three characteristic positions of the neutral line within the contact surface between the roll and the workpiece are possible.

Comparison of Calculated Values of the Actual and Effective Rolling Radii

It was established by calculation that at real values of the friction coefficient during plugless rolling ($f > 0.25$ [7]), the value of f hardly affects the ratio U (Fig. 4).

The ratio U is hardly dependent on the number of rolls forming the pass (Fig. 5). If the resultant external axial force Q is directed along rolling ($Q < 0$), the value of Q hardly affects the ratio U . If the resultant

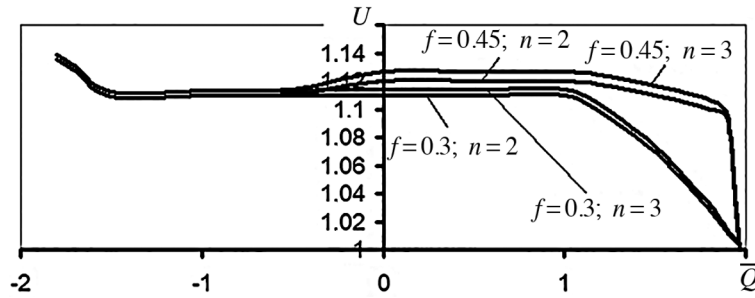


Fig. 5. Curves $U = U(\bar{Q}, f, n)$ for $\lambda_p = 1.15$, $\bar{T} = 0.45$.

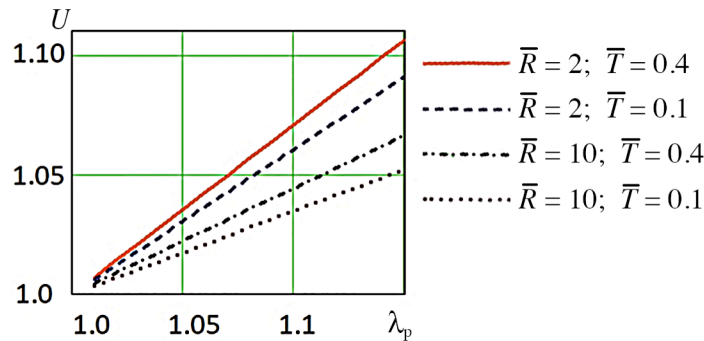


Fig. 6. Curves $U = U(\lambda_p, \bar{T})$ for $f = 0.375$, $\bar{Q} = 0$, $n = 2$.

external axial force Q is opposite to the rolling direction ($Q < 0$), increasing Q reduces the difference between the actual and effective rolling radii (Fig. 5). The ratio U increases with the ovality λ_p of the pass and the relative wall thickness \bar{T} (Fig. 6). The ratio U decreases with increase in the relative roll radius \bar{R} (see Fig. 6).

Processing the calculated data using the algorithm from [8], we obtained the following expression of the best-fit line:

$$U = 1 + (\lambda_p - 1) \cdot (0.3216 \cdot \bar{T} + 0.739) \cdot (\bar{R})^{0.1856 \bar{T} - 0.3659} \tag{11}$$

For practical purposes, the effective rolling radius is usually determined as the roll radius averaged over the pass width [9, 10]:

$$R_{\text{roly}} = R_i - R_{\text{pav}}, \tag{12}$$

where

$$R_{\text{pav}} = \frac{n}{\pi} \int_0^{z_{\text{max}}} \sqrt{1 + \left[\frac{d(\sqrt{R_{\text{pz}}^2 - z^2})}{dz} \right]^2} dz$$

is the mean radius of the roll pass.

Thus, if the effective rolling radius is defined by (12), then formula (11) can be used to determine the actual rolling radius by the formula $R_{\text{rol}} = UR_{\text{rol e}}$.

The results of the present study were used to calculate the rolling speed in the sizing and reducing mills of the Interpipe NTRP and Interpipe Niko Tube Companies.

CONCLUSIONS

1. We have developed a generalized method for calculating the rolling radius R_{rol} based on an analysis of the real form of the neutral line in the deformation zone provided that the workpiece is in equilibrium under the forces applied to it.
2. It has been established that there can be four characteristic positions of the neutral line on the contact surface between the rolls and the metal.
3. The case where the neutral line lies in a plane parallel to the rolling axis and the rolling radius is effective has been considered.
4. The actual, R_{rol} , and effective, $R_{\text{rol e}}$, rolling radii for oval roll passes have been calculated and compared.
5. A best-fit line for correcting the calculated values of the effective rolling radius has been obtained.

REFERENCES

1. Yu. G. Gulyaev, E. I. Shifrin, and N. Yu. Kvitka, "Mathematical model of continuous longitudinal plugless rolling of pipes," *Teor. Prakt. Metallurg.*, No. 6, 63–70 (2006).
2. V. N. Danchenko, A. N. Kolikov, B. A. Romantsev, and S. V. Samusev, *Pipe and Tube Production Technology* [in Russian], Intermet Engineering, Moscow (2002).
3. B. A. Romantsev, A. V. Goncharuk, N. M. Vavilkin, and S. V. Samusev, *Metal Forming* [in Russian], ID MISiS, Moscow (2008).
4. A. P. Chekmarev and Ya. L. Vatin, *Basics of Pipe Rolling in Round Roll Passes* [in Russian], Metallurgizdat, Moscow (1962).
5. *Study of Pipe Stretch-Reduction Process* [in Russian], Research Report No. 11-56-1, Acc. No. HP-573, All-Union Research and Design Institute of Metallurgical Engineering; Ukrainian Research and Design-Technology Institute of Pipe Industry, Dnepropetrovsk–Moscow (1956).
6. V. N. Danchenko, V. A. Grinkevich, and A. N. Golovko, *Metal Forming Theory* [in Russian], Porogi, Dnepropetrovsk (2010).
7. Yu. G. Gulyaev, G. I. Gulyaev, V. M. Druyan, et al., *Method for Determining the Coefficient of External Friction in Longitudinal Plugless Rolling of Pipes* [in Russian], Inventor's Certificate No. 1731309 USSR, IPC B21B 17/14; appl. June 26 1989; publ. May 7, 1992, Byull. No. 17.
8. Yu. G. Gulyaev, E. A. Maksimova, M. Z. Volodarskii, and A. G. Karpov, "An algorithm for statistical processing of empirical data," *Dokl. AN USSR, Ser. A*, No. 5, 65–68 (1985).
9. G. A. Orlov, *Basic Theory of Tube Rolling and Drawing*, Izd. Ural. Univ., Ekaterinburg (2016).
10. G. Gulyaev and Y. Gulyaev, "The mean and local wall thickness change in tubes during their reducing and sizing," in: *Proc. 42nd Mechanical Working and Steel Processing Conf.*, Vol. XXXVIII, Toronto, Ontario, Canada (2000), pp. 883–894.
11. Yu. G. Gulyaev, E. I. Shifrin, and Yu. N. Nikolaenko, "Analysis of the biting conditions in longitudinal rolling in round roll passes," in: *Proc. 10th Int. Conf. "Young Scientists 2019 – from Theory to Practice* [in Russian], NMetAU, Dnepr (2019), pp. 24–27.
12. Yu. G. Gulyaev, E. I. Shifrin, and Ya. V. Frolov, "Analyzing the contact conditions in longitudinal rolling in round roll passes," *Stal'*, No. 11, 38–41 (2019).